Journal of Korean Association of Crystal Growth
Vol. 8, No. 4 (1998) 567-572

Structural characterization of $LaTi_{0.8}V_{0.2}O_3$ compounds by transmission electron microscopy

J.Y. Kim, E.J. Yun*, K.S. Park**, K.H. Shim***, S.Y. Ryou**** and Y.H. Kim*****

Department of Materials Engineering, Hoseo University, Asan 336-795, Korea
**Department of Electrical, Electronics and Control Engineering, Hoseo University, Asan 336-795, Korea*
***Department of Materials Science and Engineering, Chung-Ju National University, Chungju 380-702, Korea*
****Electronics and Telecommunications Research Institute, Semiconductor Division, Yusong 305-350, Korea*
*****Department of Materials Science and Engineering, Sunmoon University, Asan 336-840, Korea*
******Department of Chemistry, Dankook University, Cheonan 330-714, Korea*

투과전자현미경에 의한 $LaTi_{0.8}V_{0.2}O_3$ 화합물의 결정구조 분석

김좌연, 윤의중*, 박경순, 심규환***, 류선윤****, 김유혁*****

호서대학교 재료공학과, 아산, 336-795
*호서대학교 전기전자제어공학과, 아산, 336-795
**충주산업대학교 재료공학과, 충주, 380-702
***한국전자통신연구원 반도체연구소, 유성, 305-350
****선문대학교 재료공학과, 아산, 336-840
*****단국대학교 화학과, 천안, 330-714

Abstract The crystalline structure of $LaTi_{0.8}V_{0.2}O_3$ solid solutions, prepared by arc-melting palletized mixtures of predried La_2O_3, V_2O_3, TiO_2, and Ti, was investigated by transmission electron microscopy and computer image simulation. Computer image simulations were performed by the multislice method for a wide range of sample thickness and defocusing value. The structure of $LaTi_{0.8}V_{0.2}O_3$ was determined as a $GdFeO_3$-type orthorhombic ($a \approx 5.58$ Å, $b \approx 7.89$ Å, and $c \approx 5.58$ Å) with a space group P_{nma}. No evidence of ordering of Ti and V atoms in $LaTi_{0.8}V_{0.2}O_3$ was found.

요 약 아크 용융을 사용하여, 예비 건조된 La_2O_3, V_2O_3, TiO_2, Ti의 혼합물로부터 제조된 $LaTi_{0.8}V_{0.2}O_3$ 고용체의 결정구조를 투과전자현미경과 컴퓨터 이미지 시뮬레이션을 이용하여 연구하였다. 컴퓨터 이미지 시뮬레이션은 multislice 방법으로 여러 시편 두께와 초점 거리에서 실시하였다. $LaTi_{0.8}V_{0.2}O_3$의 결정구조는 P_{nma} 공간군을 가진 $GdFeO_3$ 형태의 사방정계($a \approx 5.58$ Å, $b \approx 7.89$ Å, and $c \approx 5.58$ Å)로 결정되었다. $LaTi_{0.8}V_{0.2}O_3$에서 Ti와 V 원자의 규칙화에 대한 증거를 찾아 볼 수 없었다.

1. Introduction

The study of metal-insulator (M-I) transitions in transition-metal oxide systems is of very attractive to scientists [1]. $LaTi_{1-x}V_xO_3$ is an unusual perovskite-related compound because the antiferromagnetic ordering of the end members, $LaTiO_3$ and $LaVO_3$, is disrupted and the metal-like conductivity is observed for concentration in the range $0.10 \leq x \leq 0.25$ [2]. $LaTiO_3$ was first reported in 1954 [3] but it was not until 1979 that its structure was determined as the $GdFeO_3$-type orthorhombic structure with a space group P_{nma} by the X-ray diffraction (XRD) studies from a melt-grown, highly twinned crystal [4]. At present, it is established that $LaTiO_3$ is a semiconductor with a band gap of 0.01 eV [5], and that $LaTiO_3$ with an oxygen content of 3.0 is paramagnetic [6] or canted antiferromagnetic with a metal (M)-insulator (I) transition at 125 K [7]. There are several different reports about the crystal structure of $LaVO_3$, i.e., cubic perovskite structure [8], tetragonally distorted perovskite structure [9],

hexagonal distortion of the cubic perovskite structure [10], and isostructural to $LaTiO_3$ with the orthorhombic $GdFeO_3$-type structure (space group P_{nma}) [11]. Despite of the discrepancy in the crystal structures, it is agreed that $LaVO_3$ is a semiconductor with a band gap of 0.14 eV [9].

It is not obvious why solid solutions of antiferromagnetic $LaTiO_3$ and $LaVO_3$ would give metal-like conductivity. This is especially surprising for B-site-substituted transition metal oxide systems. Formation of solid solutions through disordered substitutions on perovskite B sites in metallic ABO_3 phases (B = transition metal) invariably localizes electrons and results in insulating behavior [12, 13]. It is suspected that it could take place in two cases. First, if these compounds have a orthorhombic or tetragonal structure of lower symmetry, the ordering of Ti and V atoms within discrete layers of the unit cell could account for the unexpected loss of magnetic ordering and onset of metallic conductivity. Second, for rare earth oxide compounds, physical properties depend strongly on the size of the rare earth ion [14] or may be structurally controlled [15]. M-I transitions are associated with the change in structural parameters such as metal-oxide (M-O) distance or metal-oxide-metal (M-O-M) angle. The structural parameters control the band width of valence and conduction bands, and thus directly affect the ratio of electron correlationship energy to band width and ultimately the transport properties. In this work, We describe the structural properties of $LaTi_{0.8}V_{0.2}O_3$ phase for explain of an unusual M-I transition in the $LaTi_{1-x}V_xO_3$ phases. The crystalline structure of $LaTi_{0.8}V_{0.2}O_3$ was investigated by transmission electron microscopy and computer image simulation.

2. Experimental

$LaTi_{0.8}V_{0.2}O_3$ solid solutions were prepared by arc-melting palletized mixtures of predried La_2O_3, V_2O_3, TiO_2, and Ti. The oxygen contents of the mixtures were adjusted to be oxygen deficient (~1.0) to compensate for the slight oxidation in the dc arc furnace. The palletized mixtures and a button of zirconium metal were placed in separated cavities of a water-cooled copper hearth inside an arc furnace that was evacuated and purged with gettered Ar gas several times prior to the reaction. Samples were fired several times with repetitive turnings. Before each pellet was fired, the zirconium metal was melted in order to purify the atmosphere inside the furnace. The resulting phases were then pulverized in a percussion mortar and then finely ground. All single phase samples were stored in a vacuum atmosphere dry box to prevent oxidation.

Table 1
Input microscope parameters used in the computer simulation of lattice images

Operating voltage (V)	200 kV
Radius of objective aperture (r_s)	3.37 nm^{-1}
Spherical aberration coefficient (C_s)	2.3 mm
Semi-angle of illumination	1.0 mrad
Half-width of Gaussian spread of vibration	0.0 nm
Half-width of Gaussian spread of defocus	5 nm

The crystal structure of $LaTi_{0.8}V_{0.2}O_3$ was investigated by transmission electron microscopy (TEM). In order to confirm the crystal structure determined from TEM, experimental high-resolution lattice images were compared with computer simulated ones. The computer simulations of lattice images were performed using the multislice method [16-18], assuming a $GdFeO_3$-type orthorhombic structure with a space group Pnma. The sample thicknesses ranged from 50 to 200 Å with a step of 7.89 Å, and the defocusing values from -300 to -1100 Å with a step of 200 Å. The input microscope parameters used in the computer simulation of the images are given in Table 1.

3. Results and discussion

The selected area diffraction (SAD) technique was used to determine if there was ordering between the Ti and V atoms in the B sublattice, and to obtain the unit cell length and space group from several different zone axes of many different crystals. Then, it was determined if unexpected spots were the result of multiple diffraction. Diffraction due to double diffraction can be distinguished by tilting the crystal about the direction which contains the spot in question. The intensity of this spot will remain if it is an allowed reflection and it will disappear if it is due to double diffraction.

We investigated the diffraction pattern with $[10\bar{1}]$, [010], [001], [100] and $[01\bar{1}]$ zone axes. Figure 1(a)

shows a selected area diffraction (SAD) pattern from $LaTi_{0.8}V_{0.2}O_3$. This pattern can be indexed as the $[10\bar{1}]$ zone axis of an orthorhombic structure (a $\approx c \approx 5.58$ Å and $b \approx 7.89$ Å). For checking the double diffraction, systematic absences of reflections were investigated by tilting the crystal about the direction which contains the reflection in question. When the sample was tilted away from the $[10\bar{1}]$ zone axis with respect to the [010] axis, the (010) spot was disappeared as shown in Fig. 1(b). This indicates that the (010) spot is an additional spot arising from the double diffraction. In Fig. 1(b), the conditions for allowed $(0k0)$ reflections are k=even integer. When the sample was tilted away with respect to the [111] axis, the (111), (121), and (101) spots did not disappear as shown in Fig. 1(c). Therefore, these spots correspond to allowed reflections.

A different zone axis [010] of the same orthorhombic structure gave the SAD pattern shown in Fig. 2(a). The sample was tilted away from the [010] zone axis with respect to the [100], [001], and [201] axes, respectively, as shown in Figs. 2(b)-(d). The (100) and (300) spots were disappeared in Fig. 2(b), and the (001) and (003) spots were disappeared in Fig. 2(c). Hence the (100), (300),

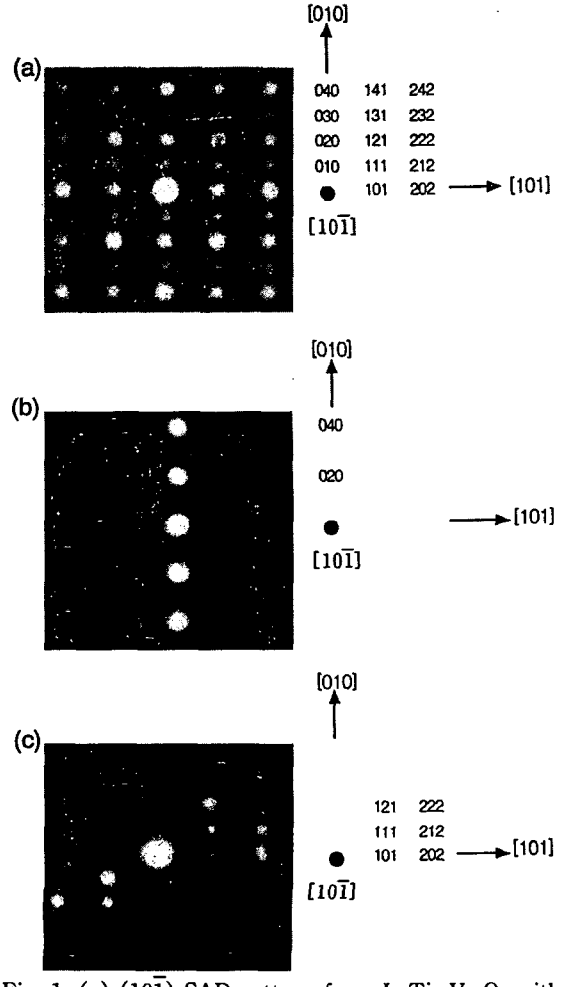

Fig. 1. (a) $(10\bar{1})$ SAD pattern from $LaTi_{0.8}V_{0.2}O_3$ with an orthorhombic structure. SAD patterns obtained from the sample tilted away from the $[10\bar{1}]$ zone axis with respect to the (b) [010] and (c) [111] axes.

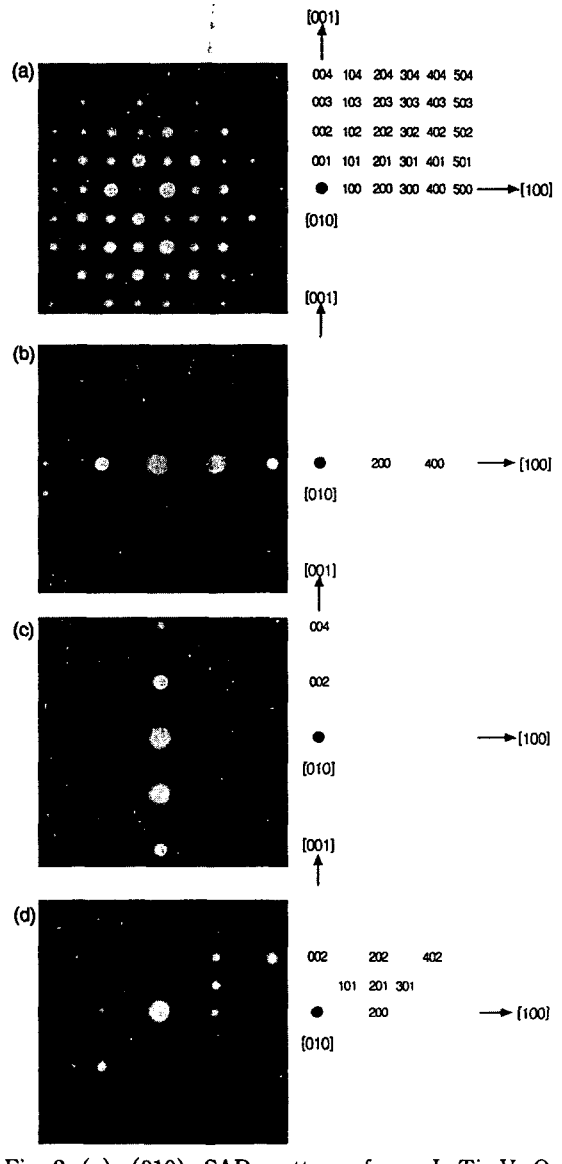

Fig. 2. (a) (010) SAD pattern from $LaTi_{0.8}V_{0.2}O_3$. SAD patterns obtained from the sample tilted away from the [010] zone axis with respect to the (b) [100], (c) [001], and (d) [201] axes.

(001), and (003) spots originated from the double diffraction. The (101), (201), and (301) spots, however, remained as shown in Fig. 2(d), indicating allowed spots. From these results, the conditions for allowed (*h00*) and (*00l*) reflections are h = even integer and l = even integer, respectively, and the conditions for allowed (*h0l*) reflections are h = even or odd integer and l = even or odd integer. Also, the patterns from the [001], [100], and [01$\bar{1}$] zone axes of $LaTi_{0.8}V_{0.2}O_3$ were obtained, as shown in Figs. 3(a)-(c). The above results indicate that the most probable structure of $LaTi_{0.8}V_{0.2}O_3$ at room temperature is $GdFeO_3$-type orthorhombic ($a \approx 5.58$ Å, $b \approx 7.89$ Å, and $c \approx 5.58$ Å) with a space group P_{nma} (reflection conditions; 0kl: k+l = even integer, hk0: h = even, h00: h = even integer, 0k0: k = even integer, 00l: l = even integer). This result agrees with the XRD and synchrotron X-ray diffraction (SXRD) data [19]. In addition, no evidence of ordering of Ti and V atoms in $LaTi_{0.8}V_{0.2}O_3$ was found (The evidence of ordering of Ti and V atoms is an additional spots in SAD pattern with a lattice parameter of $2a_p$ where $2a_p$ is the unit cell parameter). From these results, the presence of metallic

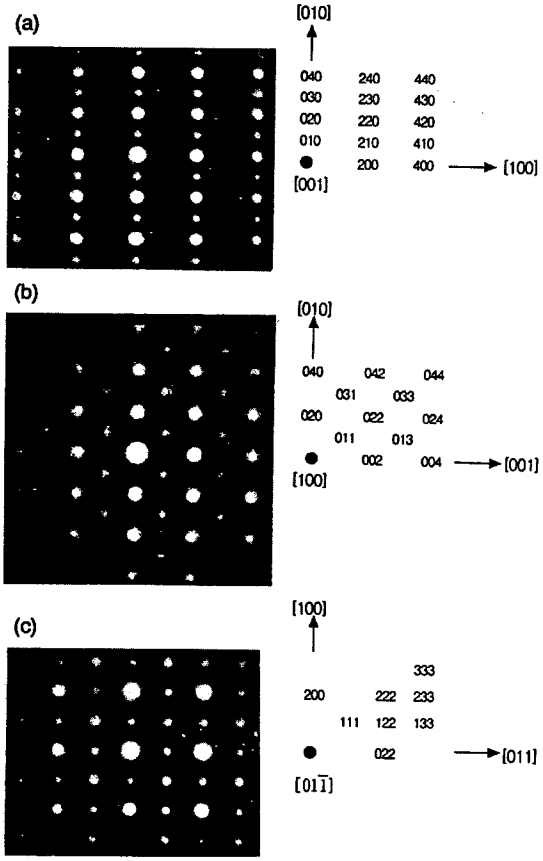

Fig. 3. (a) (001), (b) (100), and (c) (01$\bar{1}$) SAD patterns from $LaTi_{0.8}V_{0.2}O_3$.

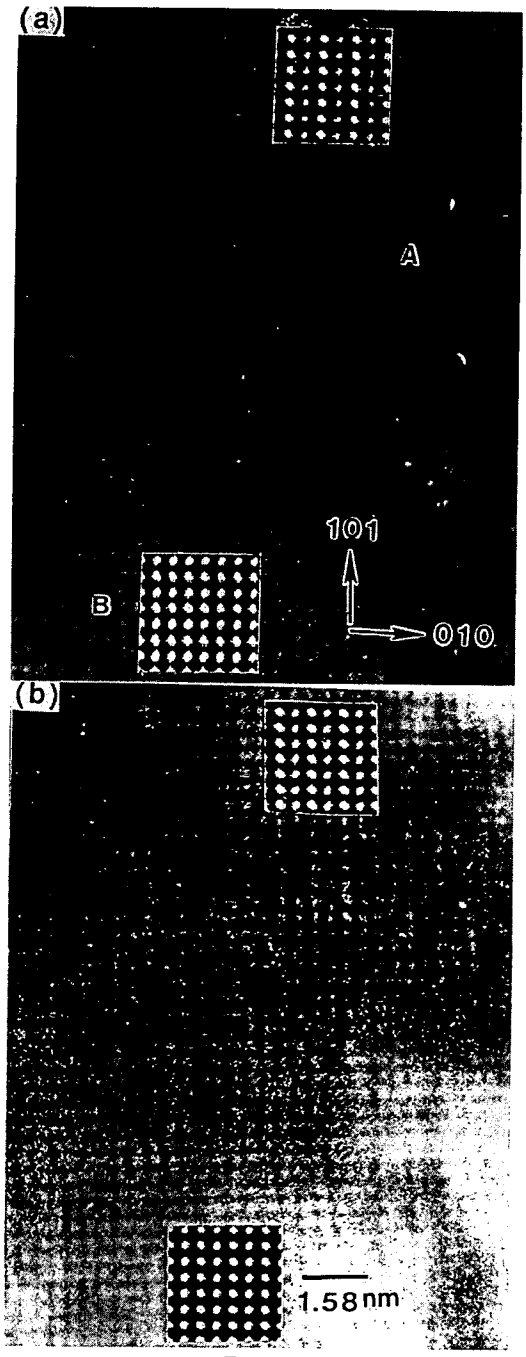

Fig. 4. Experimental (10$\bar{1}$) lattice images obtained from the same sample area under two different defocusing values, (a) -700 and (b) -900 Å.

conductivity in $LaTi_{0.8}V_{0.2}O_3$ is not obvious now. We can only suppose this behavior with the change in structurally parameters (Hubbard model) [15].

In order to confirm the orthorhombic structure of $LaTi_{0.8}V_{0.2}O_3$ determined from TEM, a visual comparison of experimental and computer simulated lattice images of $LaTi_{0.8}V_{0.2}O_3$ was carried. $(10\bar{1})$ experimental lattice images from the same sample area were obtained under two different defocusing values (Fig. 4). In Fig. 4, the periodicities along the [010] and [101] directions in area A correspond to the (010) and (101) interplannar spacings, respectively, and the periodicities along the [010] and [101] directions in area B to the (020) and (101) interplannar spacings, respectively. It is shown that the (010) spot was generated by double diffraction (see Figs. 1(a) and (b)), which contributes to the generation of the (010) lattice fringes in area A.

The computer simulations of lattice images were performed using the multislice method, assuming a $GdFeO_3$-type orthorhombic. The atomic positions and unit lengths obtained from the Rietveld refinement of neutron data are shown in Table 2. By a comparison of the experimental images (Fig. 4) and the simulated images (Fig. 5), the experimental images were in good agreement with the simulated images. The experimental images indicated by A in

Table 2
Refined structural parameters for $LaTi_{0.8}V_{0.2}O_3$ at 50 K

Atom	Site symmetry	x	y	z	B (iso)	Fraction
La	.m.	0.0344	0.25	0.9944	0.18	0.97
Ti	1	0.5	0	0	0.18	0.82
V	1	0.5	0	0	0.18	0.18
O (1)	.m.	0.0886	0.25	0.0771	0.69	1.09
O (2)	1	0.2862	0.344	0.7142	0.77	0.99

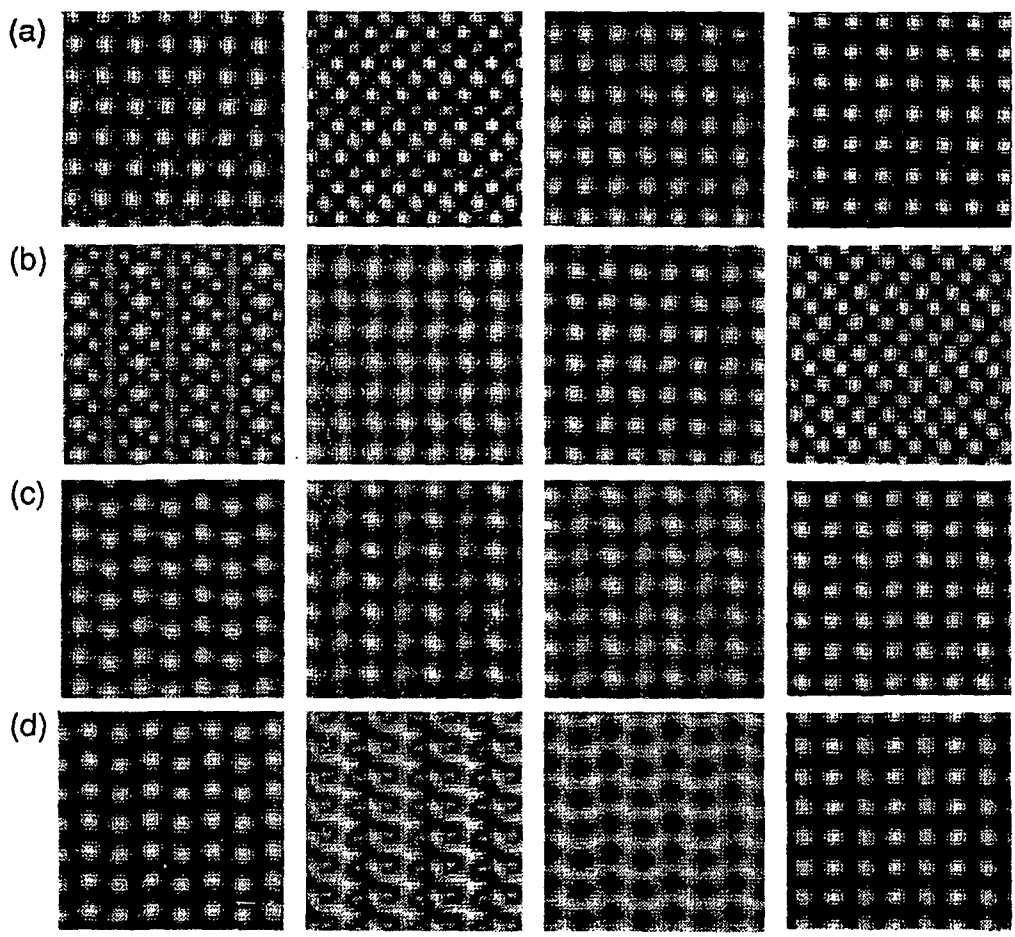

Fig. 5. $(10\bar{1})$ simulated lattice images from $LaTi_{0.8}V_{0.2}O_3$ with a sample thickness of (a) 94.8, (b) 126.4, (c) 158.0, and (d) 189.6 Å. (The defocusing values for each column are, from left to right, $\Delta f = -500, -700, -900$, and -1100 Å).

Figs. 4(a) and (b) are well matched with the simulated images obtained -700 and -900 Å defocusing values, respectively, at 158 Å sample thickness. Also, the experimental images indicated by B in Figs. 4(a) and (b) are well matched with the simulated images obtained -700 and -900 Å defocusing values, respectively, at 126 Å sample thickness. The good agreement between the experimental and simulated images confirms that $LaTi_{0.8}V_{0.2}O_3$ compound has a $GdFeO_3$-type orthorhombic ($a \approx 5.58$ Å, $b \approx 7.89$ Å, and $c \approx 5.58$ Å) with a space group P_{nma}.

Acknowledgements

This work was supported by the Korea Science and Engineering Foundation (KOSEF) through the Semiconductor Equipment Research Center at Hoseo University.

References

[1] N. Mott, Metal-Insulator Transitions, 2nd ed. (Tayler and Francis, New York, 1990).
[2] C. Eylem, Ph. D. Dissertation, University of Maryland, U.S.A, (1995).
[3] M. Kestigian and R. Ward, J. Am. Chem. Soc. 76 (1954) 6027.
[4] D.A. MacLean, H.K. Ng and J.E. Greedan, J. Solid State Chem. 30 (1979) 35.
[5] F. Lichtenberg, D. Widmer, J.G. Bednorz, T. Williams and A. Reller, Z. Phys. B82 (1991) 211.
[6] D.B. Rogers, A. Ferretti, D.H. Ridgley, R.J. Arnott and J.B. Goodenenough, J. Appl. Phys. 37 (1966) 1431.
[7] J.T. Vaughey, J.P. Thiel, E.F. Hasty, D.A. Groenke, C.L. Stem, K.R. Poeppelmeier, B. Dabrowski, D.G. Hinks and A.W. Mitchell, Chem. Mater. 3 (1991) 935.
[8] P. Doughler and P. Hagenmuller, J. Solid State Chem. 11 (1974) 177.
[9] A.V. Mahajan, D.C. Johnston, D.R. Torgeson and F. Borsa, Phys. Rev. B46 (1991) 10966.
[10] P. Dougler and A.J. Casalot, J. Solid State Chem. 2 (1970) 396.
[11] P. Bordet, C. Chaillout, M. Marezio, Q. Huang, A. Santoro, S.-W. Cheong, H. Takagi, C.S. Oglesby and B.J. Batlogg, J. Solid State Chem. 106 (1993) 253.
[12] R.J. Bouchard, J.F. Weiher and J.L. Gillson, J. Solid State Chem. 6 (1990) 135.
[13] C.N. Rao, Annu. Rev. Phys. Chem. 40 (1989) 291.
[14] J.E. Greedan and D.A. Maclean, Inst. Phys. Conf. Ser. 37 (1978) 249.
[15] J.B. Goodenough, Progr. Solid State Chem. 5 (1971) 315.
[16] J.M. Cowley and A.F. Moodie, Acta Crystallogr. 10 (1957), 609.
[17] J.M. Cowley and A.F. Moodie, Acta Crystallogr. 12 (1959) 353.
[18] J.M. Cowley and A.F. Moodie, Acta Crystallogr. 12 (1959) 360.
[19] C. Eylem, Y.-C. Hung, H.L. Ju, J.Y. Kim, D.C. Green, T. Voget, J.A. Hriljac, B.W. Eichhorn, R. L. Greene and L. Salamanca-Riba, Chem. Mater. 8 (1996) 418.